



## Direct measurement of the time-dependent mechanical response of HPMC and PEO compacts during swelling

Kathryn Otim Hewlett<sup>a</sup>, Jennifer L'Hote-Gaston<sup>b</sup>, Michael Radler<sup>b</sup>, Kenneth R. Shull<sup>a,\*</sup>

<sup>a</sup> Department of Materials Science and Engineering, Northwestern University, Evanston, IL 60208, United States

<sup>b</sup> Dow Wolff Cellulosics R&D, The Dow Chemical Company, Midland, MI 48674, United States

### ARTICLE INFO

#### Article history:

Received 20 December 2011

Received in revised form 12 April 2012

Accepted 1 May 2012

Available online 15 May 2012

#### Keywords:

Mechanical properties

Drug release compacts

Indentation

### ABSTRACT

Mechanical indentation is used to measure the time dependent mechanical properties of three model compact formulations during swelling in aqueous media. The formulations are based on polyethylene oxide (PEO), hydroxypropyl methylcellulose (HPMC) and a PEO/HPMC blend. The technique is sensitive to changes in compact thickness and mechanical response and is used to characterize changes in the mechanical properties of the model compacts during the swelling process. The gel thickness and the effective elastic modulus of the gel layer are obtained from the load/displacement relationship during initial indentation. The HPMC and hybrid compacts showed significantly more swelling (110%) than the PEO compact (67%). Viscoelastic properties of the gel layer are determined throughout the swelling process by an oscillatory indentation method. Results show the complex modulus of all three compacts decreasing by approximately an order of magnitude over the course of swelling for 6 h. The measurement techniques presented here can easily be extended to more complex systems.

© 2012 Elsevier B.V. All rights reserved.

### 1. Introduction

In a controlled-release compact, a compacted glassy or semicrystalline polymer with a molecular weight well above the entanglement molecular weight is embedded with a drug and other excipients. Upon exposure to liquid the matrix undergoes a transition to a rubbery regime, accompanied by swelling and, in many cases, eventual dissolution. During the initial stages of swelling a thin gel layer is formed at the surface of the compact. Over time water diffuses through this gel layer into the compact core and the polymer chains continue to swell. This time-dependent swelling process is used to modulate release of the drug from the polymer matrix. The drug release profile from these matrices can be altered by changing the polymer's composition and molecular weight (Jamzad et al., 2005; Li and Gu, 2007). While there are many factors (e.g. pH and hydrophilicity of the drug) that contribute to the drug release profile, gel layer thickness has been shown to be one of the most important (Efentakis et al., 2007; Yang et al., 1998). The mechanical properties of this gel layer are directly relevant to in vivo performance because the gel is subjected to contractile forces exerted by the stomach and intestine. In addition, accurate characterization of the structure and mechanical response of the

polymer gel layer can enhance understanding of the matrix behavior and aid in the control of drug release profiles.

The swelling process can generally be characterized by three regimes: initial swelling, front motion, and dissolution (Harland et al., 1988; Yang et al., 1998). In the initial swelling regime a penetration front is established, defined as the interface between a swollen, rubbery gel layer and a glassy or semicrystalline core (Jamzad et al., 2005; Sung et al., 1996). Because solvent diffusion in the rubbery portion of the sample is much faster than the diffusion in the core, the penetration front moves at a constant velocity in a phenomenon referred to as case II diffusion (Gall et al., 1990; Thomas and Windle, 1978). The dissolution front (often referred to in the literature as an erosion front) is the border between the swollen gel and the medium in which it is immersed. In the front motion regime, the gel layer thickness is determined by the relative velocities of the penetration and dissolution fronts. Dissolution occurs when the outer portion of the gel has decreased to a critical concentration, where the polymer chains are no longer entangled and are free to migrate into the solution. For very high molecular weight polymers, the kinetics of dissolution are slowed by the presence of intermolecular entanglements, so that a transient viscoelastic polymer gel is formed prior to complete dissolution of the polymer (Efentakis et al., 2007; Kavanagh and Corrigan, 2004; Li and Gu, 2007; Maggi et al., 2002; Yang et al., 1998).

The interrelated processes of drug diffusion, polymer swelling, and dissolution create a very complex system that is difficult to analyze. A focus of previous research has been to correlate swelling

\* Corresponding author. Tel.: +1 847 467 1752; fax: +1 847 491 7820.  
E-mail address: [k-shull@northwestern.edu](mailto:k-shull@northwestern.edu) (K.R. Shull).

**Table 1**  
List of compact formulations.

Formulation	Component	Concen. (wt%)	Hardness (SCU/N)	Thickness (mm)	Weight (mg)
HPMC	HPMC	97.7	37 ± 2.7/259 ± 19	4.35 ± 0.05	384.55 ± 7.39
	Silica	1.8			
	Magnesium stearate	0.5			
PEO	PEO	99.5	47 ± 2.5/329 ± 18	4.51 ± 0.02	395.08 ± 2.85
	Magnesium stearate	0.5			
	HPMC	32.9			
PEO/HPMC	PEO	66	36 ± 1.7/252 ± 12	4.56 ± 0.07	401.64 ± 6.14
	Silica	0.6			
	Magnesium stearate	0.5			

behavior with the corresponding drug release profiles (Abrahmsen-Alami et al., 2007; Conti et al., 2007a; Durig and Fassihi, 2002; Efentakis et al., 2007; Jamzad et al., 2005; Ju et al., 1995; Kavanagh and Corrigan, 2004; Li and Gu, 2007; Maggi et al., 2002; Reynolds et al., 1998; Wan et al., 1995; Wu et al., 2005; Yang et al., 1998). A variety of imaging techniques, including optical microscopy and NMR, have been used to observe how the compacts swell over time (Abrahmsen-Alami et al., 2007; Adler et al., 1999; Colombo et al., 1999; Conti et al., 2007b; Efentakis et al., 2007). Optical microscopy has the advantage of being a simple technique for determining the size and location of the compact layers. NMR provides high resolution images of the local variations within the swollen region, but the experiments can be time consuming. With these techniques the swelling and dissolution fronts have been observed (Colombo et al., 1999). Magnetic resonance imaging and X-ray microtomography have also been used to analyze compact swelling (Chen et al., 2010; Laity and Cameron, 2010; Laity et al., 2010; Mikac et al., 2010).

While the imaging methods described above can provide information about the kinetics of formation and dissolution of the gel layer, they do not provide any information about the mechanical properties of this layer. This information is commonly obtained by indentation, often referred to as texture analysis in the drug release literature (Durig and Fassihi, 2002; Jamzad et al., 2005; Li and Gu, 2007; Yang et al., 1998). In a conventional texture analysis experiment, a compact is compressed by a 2-mm diameter punch to a load of 2–40 N (Conti et al., 2007a; Jamzad et al., 2005; Li and Gu, 2007; Yang et al., 1998). At these loads the probe is able to penetrate the glassy core of the compact. Integration of the force–displacement curve provides a measure of the work of penetration. Indentation experiments have also been used to measure the mechanical properties of polymers and other soft materials, using smaller loads and a smaller punch diameter so that the elastic properties of the gel are obtained (Lin et al., 2009; Shull, 2002; Shull et al., 1998).

In the work presented in this paper, we use indentation to measure the mechanical response of the gel layer of polyethylene oxide (PEO), hydroxypropyl methylcellulose (HPMC) and PEO/HPMC blend compacts as a function of hydration time. These indentation experiments allow us to observe the properties of a single compact over time, using a small punch size to obtain a sensitive measure of the depth-dependent mechanical properties. We focus on the forces and behavior observed up to the point of initial contact with the glassy core rather than the force required to penetrate the core. At long swelling times, we are able to probe behavior of the gel layer itself, independent of the glassy core. Our experimental protocol is described below, followed by a description of the results obtained for the three different compacts.

## 2. Experimental

### 2.1. Materials

Hydroxypropyl methylcellulose (HPMC, METHOCEL™ K100 M Premium cellulose ether) and polyethylene oxide (PEO, POLYOX™ 301 NF water soluble resin) were supplied by The Dow Chemical Company (Midland, MI). Silica was supplied by Spectrum Chemical & Laboratory Products (Gardena, CA). Magnesium stearate (NF) was supplied by Mallinckrodt (Hobart, NY).

Compacts were formed with the compositions listed in Table 1. POLYOX typically contains silica, which serves as a flow aid and is added during the production process. Additional silica was added to formulations containing HPMC to be consistent with the silica content of the PEO (~1.8 wt%) and to increase powder flow properties of HPMC through the hopper during compaction. Magnesium stearate was added as a lubricant. A hydrochloric acid buffer of pH 1.2 ± 0.1 was prepared according to standard U.S. Pharmacopeia methods (Formulary, 2009). The buffer contained hydrochloric acid and potassium chloride, which were both supplied by Mallinckrodt. The

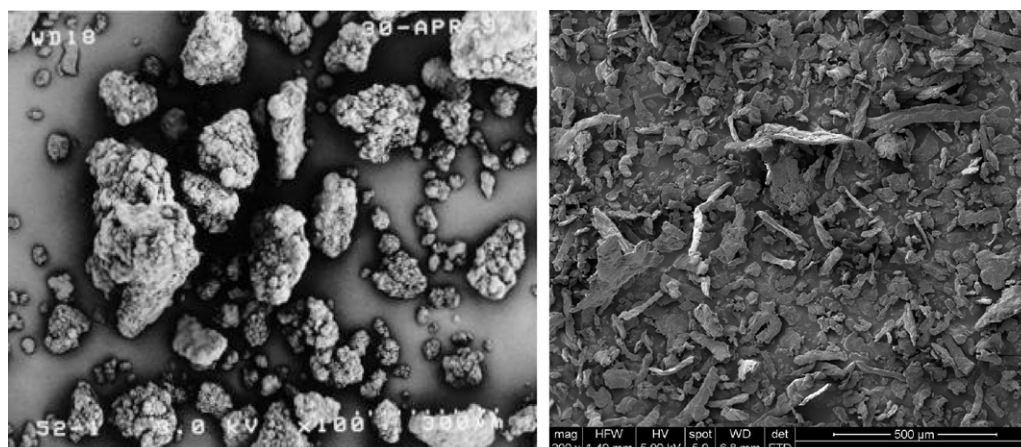


Fig. 1. SEM images of PEO (left) and HPMC (right) powders.

molecular weights of the polymers were characterized by viscosity measurements, and give a viscosity-average molecular weight,  $M_v$ . The PEO used in these experiments has  $M_v \sim 4,000,000$  g/mol and HPMC has  $M_v \sim 100,000$  g/mol. The bulk density of HPMC is 1.326 g/cc and PEO is 1.3 g/cc. The general polymer morphology is shown in Fig. 1. PEO has a more spherical shape while HPMC forms fibrous aggregates.

## 2.2. Compact formulation and hardness

Dry powders were blended in a 16-quart V-blender and mixed for 10 min. Magnesium stearate was then added and subsequently blended for an additional minute. The homogenized blend was then transferred to a mass-flow hopper. Solid compacts weighing 400 mg were prepared by direct compression using a 16-station Manesty Beta compact press equipped with 0.4063 in. (10.3 mm), flat-faced, bevel-edge tooling at a compression force of 4000 lb and a speed of 12–15 rpm. The resulting compacts have a diameter of 10.3 mm and an average thickness of 4.5 mm. Compact hardness (crushing strength) was measured using a Key Hardness Tester (Key International, Elizabethtown, New Jersey). The hardness tester is based on the Strong-Cobb tester, which compresses a compact in the radial direction until it breaks (Ridgway, 1970). Hardness values for the dry compacts listed in Table 1 are reported in Strong-Cobb units (SCU) and in Newtons, with 1 SCU = 7 N.

## 2.3. Indentation measurements

A schematic of the indentation setup is shown in Fig. 2. A flat-bottomed cylindrical punch of radius 0.44 mm was attached to a 50 g load cell and inchworm motor. A fiber optic sensor measured displacement of the punch while a side-view camera provided optional imaging. The instrument was controlled externally via a computer. Time-dependent swelling experiments used LabView software (National Instruments Corp., Austin, TX), while the oscillatory indentation used an updated version of the program in MATLAB (Mathworks, Natick, MA).

Indentation experiments were typically performed by immersing the samples in  $\sim 20$  mL of 1.2 pH HCl buffer maintained at  $37 \pm 0.5$  °C. This buffer was chosen to represent the acidic conditions experienced by drug delivery dosage forms in the stomach. A side view camera was used to image the compacts during the experiments. Each compact was glued to a glass slide using superglue to prevent lateral movement during measurements. The compact and slide were placed in a deep glass dish containing preheated HCl buffer solution. The slide was weighed down to reduce vertical movement of the compact. The dish was surrounded by a copper block that was heated externally to maintain a constant solution temperature. The compact remained submerged during experiments, and the sample dish was covered between tests to reduce solvent evaporation. Fig. 3 shows representative images as an HPMC compact as it swells in water.

In a typical set of experiments, a single compact was immersed in solution for up to 7 h. Measurements were taken multiple times during the first hour and then hourly after that. The punch was left out of contact with the sample in between indentations so

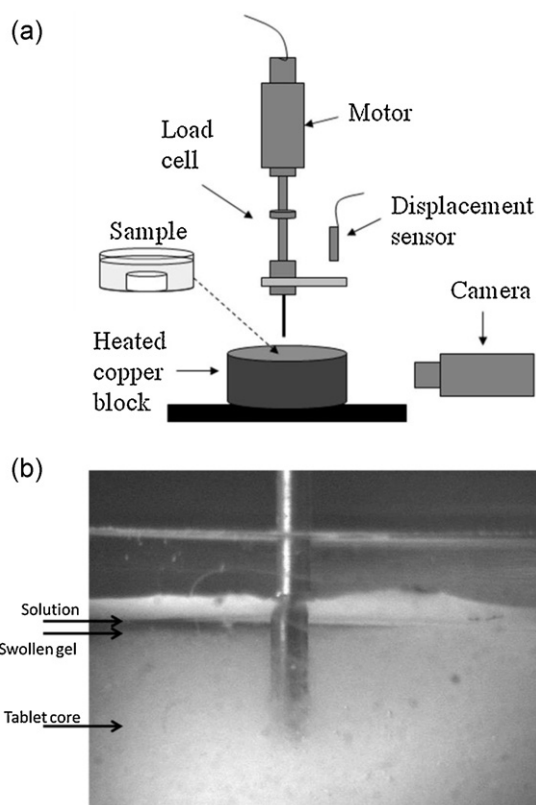


Fig. 2. Indentation setup (a), and representative image obtained during indentation of a swollen sample (b).

that the sample could swell freely. The compact was rotated in between indentations so that each test was not affected by previous measurements. In a standard indentation experiment the punch was advanced into contact with the compact until a specified load, ranging from 25 to 250 mN, was reached. The resulting load and displacement data were used to compare the effective elastic modulus and gel thickness during the swelling and gelation processes. We defined an effective modulus,  $E_{\text{eff}}$ , from the slope of the stress–displacement curve at a stress of 10 kPa, using the expression for the indentation of an elastic half space with a cylindrical punch (Sneddon, 1965):

$$E_{\text{eff}} = \frac{3}{8a} \left( \frac{dP}{d\delta} \right) = \frac{3\pi a}{8} \left( \frac{d\sigma_{\text{avg}}}{d\delta} \right) \quad (1)$$

In this expression,  $a$  represents the punch radius and  $\delta$  the displacement. The load,  $P$ , and stress,  $\sigma_{\text{avg}}$ , are related by this radius:

$$\sigma_{\text{avg}} = \frac{P}{\pi a^2} \quad (2)$$

The effective thickness,  $h_{\text{eff}}$ , corresponds to the displacement at the point where the effective modulus was calculated. Fig. 4 is an example of a curve used to define the effective modulus and effective thickness.



Fig. 3. Images of a dry HPMC compact and the same compact after swelling for 30 min, 1 h, 6 h, and 15 h. The dry compact diameter is 10.3 mm.

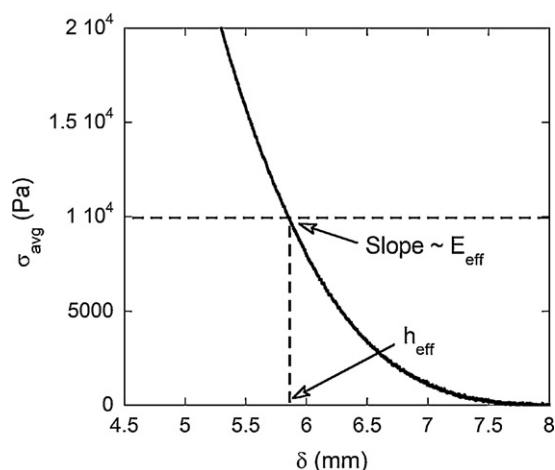


**Fig. 4.** Sample curve used to calculate the effective modulus and thickness. The effective modulus ( $E_{\text{eff}}$ ) is the slope of the curve at a stress of 10 kPa and the effective thickness ( $h_{\text{eff}}$ ) is the displacement at the point where  $E_{\text{eff}}$  is calculated.

#### 2.4. Oscillatory indentation

Dynamic mechanical measurements, where the response to an oscillatory applied displacement is measured, are often used to characterize the behavior of viscoelastic materials similar to the gel layers investigated here. In order to illustrate the ability to obtain dynamic mechanical information during swelling, we have applied an oscillatory indentation test to the swollen compacts. In these experiments, the indenter was advanced into contact with a sample that had been immersed in room temperature deionized water. Once a specified load was reached, the indenter velocity was oscillated sinusoidally with a peak-to-peak amplitude of 25  $\mu\text{m}$  at a frequency of 1 Hz. The measured loads prior to beginning of the oscillatory portion of the test ranged from 15 mN to 100 mN (stresses of 34–226 kPa). Higher loads were used at shorter hydration times and lower loads used at longer hydration times as the compacts softened considerably at the longer hydration times. Fig. 5 shows a typical load–displacement curve, in which the sample is pre-loaded to a given value and the indenter is oscillated before being retracted to the starting position.

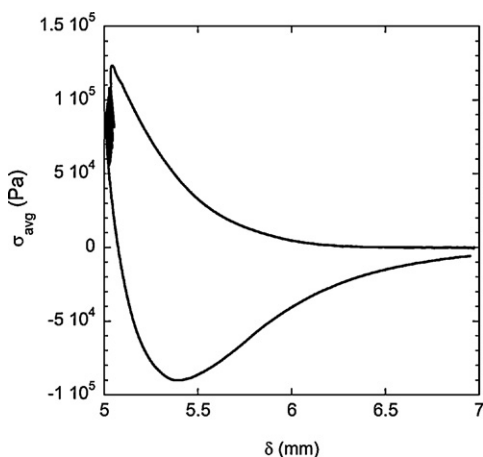


**Fig. 5.** Load–displacement curve of a typical oscillatory indentation experiment in which the sample is pre-loaded before the oscillations begin. The curve presented here is for an HPMC compact after 2 h of swelling.

The load,  $P$ , and displacement,  $\delta$ , are functions of the phase angle,  $\Delta$ , which is calculated by integrating the area in a single cycle:

$$\begin{aligned} \delta &= \delta_0 \sin(\omega t) \\ P &= P_0 \sin(\omega t - \Delta) \\ \sin(\Delta) &= \frac{\int P d\delta}{\pi P_0 \delta_0} \end{aligned} \quad (3)$$

In these equations  $\omega$  is the applied angular frequency (Crosby et al., 2002). The complex elastic modulus,  $E^*$ , can be calculated from the measured load and displacement data. This expression is analogous to Eq. (1), but is written in terms of frequency:

$$E^*(\omega) = \frac{3\pi a \sigma_0(\omega)}{8\delta_0(\omega)} \quad (4)$$

where  $\sigma_0$  is the measured load amplitude and  $\delta_0$  is the displacement amplitude. The loss and storage moduli are simple functions of the complex modulus:

$$\begin{aligned} E' &= E^* \cos \Delta \\ E'' &= E^* \sin \Delta \end{aligned} \quad (5)$$

Fig. 6a presents the oscillatory portion of the experiment shown in Fig. 5. For a perfectly elastic material the stress–displacement curves overlap completely. The hysteresis in the data presented here is due to stress relaxation in the gel layer over the course of the oscillations. To correct for this relaxation, we can determine shift factors for the stress and displacement data with respect to time. The red circles in Fig. 6a correspond to the points that were used to calculate these shifts. Fig. 6b and c show the displacement–time and stress–time curves, respectively, and their corresponding polynomial fits. The data collapse to an ellipse (Fig. 7a) once the polynomial fits have been subtracted from the original data (Fig. 6a). These curves can then be used to determine the complex modulus and phase angle (Eqs. (3)–(5)). A sample curve used to calculate the above values is given in Fig. 7b. The phase angle is determined by integrating the shaded region.

### 3. Results and discussion

#### 3.1. Compact swelling

Fig. 8 shows the stress response of the PEO, HPMC, and PEO/HPMC compacts as a function of indenter displacement at different swelling times. These samples were tested in HCl buffer heated to 37  $^\circ\text{C}$ . The dashed line represents the top surface of a dry compact. The substrate was defined as a displacement of zero so that the displacement at initial contact would be a measure of axial swelling. The HPMC compact (Fig. 8a) showed significant swelling over time, increasing 110% (5 mm) from its initial thickness after 7 h. The amount of overall swelling in the PEO compact (Fig. 8b) was 67% (3 mm), while the PEO/HPMC compact (Fig. 8c) also swelled 5 mm (110%) after 7 h.

The results of the swelling studies and hardness performed here were summarized and compared to data available in literature to gain better insight and understanding on hydration and swelling properties of PEO and HPMC (Table 2). Previous results (examples 1 and 3 from Table 2) have shown that high molecular weight PEO swells to a greater degree than high molecular weight HPMC at similar hydration conditions and time, independent of the measurement technique used. Conversely, other results (examples 2 and 4 from Table 2) have shown that high molecular weight HPMC swells to a greater extent than high molecular weight PEO, primarily when hydrated in buffered solutions at similar hydration times. Additionally, the presence or lack of drug in



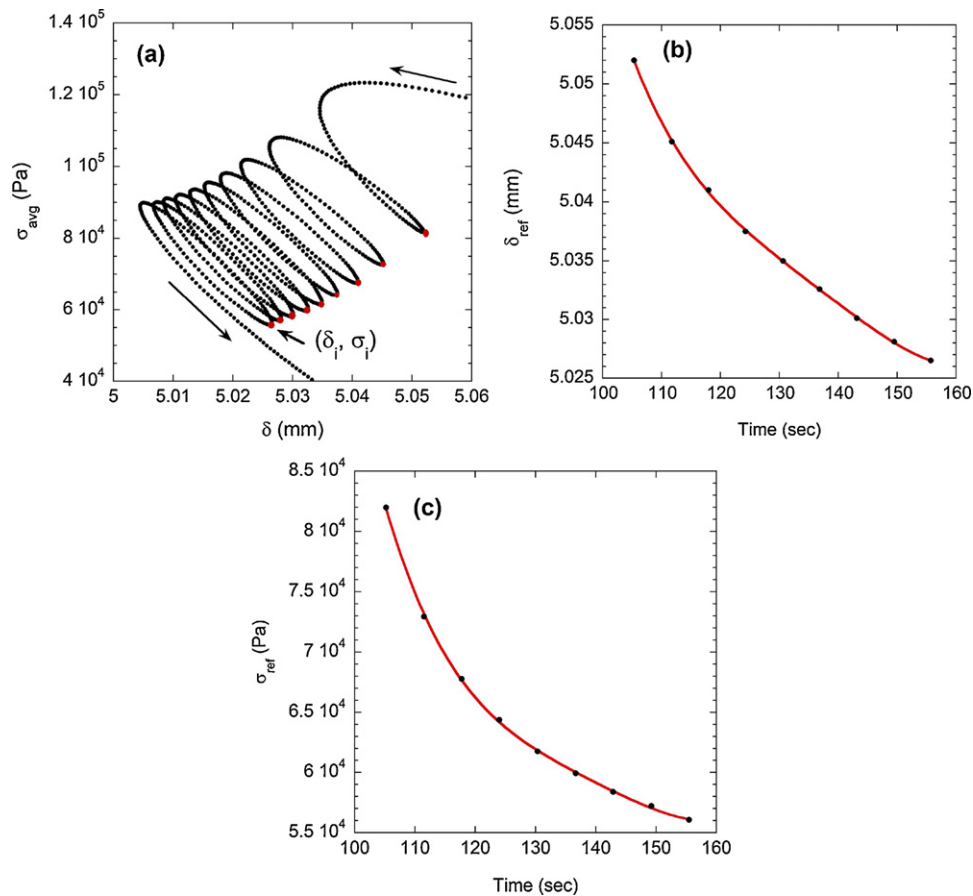


**Fig. 6.** (a) Oscillatory portion of a stress–displacement curve for an HPMC compact after 2 h of swelling. The sample was loaded to 34 kPa before the oscillations began. The red circles indicate points that were used to calculate polynomial shifts of load and displacement as functions of time (b and c).

the compact does not appear to have a significant effect on either the swelling performance or the relative differences in tablet hardness. Because of the lack of available information on the hardness properties in example 3 and compression conditions in examples 1 and 2, it is difficult to draw any significant conclusions regarding the influence of hardness on swelling performance for these polymers.

The differences in swelling behavior and performance of the various examples summarized in Table 2 may be explained by further discussion concerning the hydration media used in the swelling experiments. It is well known that the presence of inorganic salts in

aqueous PEO solutions can lower the precipitation temperature and the intrinsic viscosity of PEO (Ritscher and Elias, 1959). This salting-out effect is also known to reduce the hydrodynamic volume of the polymer. The salting-out effect is not a function of ionic strength, but rather dependent on both the cation and anion, with  $K^+$  and  $HPO_4^{2-}$  ions (pH 1.2 HCl/KCl and pH 6.8 phosphate buffers, respectively) having the greatest effect on the upper temperature limits of solubility. The potential reduction in hydrodynamic volume of PEO compacts during hydration in buffered medias may explain the reduced swelling performance in examples 2 and 4 relative to HPMC compacts.

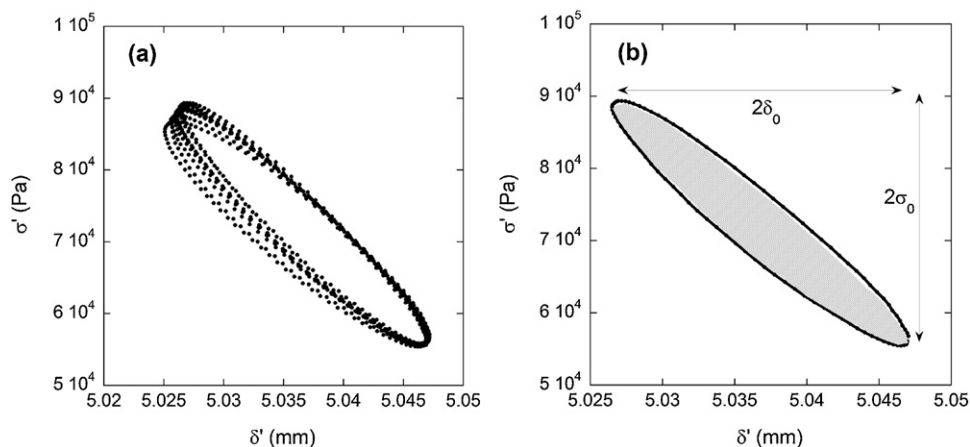


**Fig. 7.** (a) Resulting stress–displacement curve once the shifts from Fig. 6 have been applied. (b) Sample stress–displacement curve for a single cycle.

**Table 2**  
Comparison of swelling results in published literature.

Expt	Result	Technique	Media	Swelling at 8 h	HPMC	HPMC hardness	PEO	PEO hardness	Drug	Ref.
1	PEO > HPMC	Tablet volume	DI water	2900/1900 mm <sup>3a</sup>	K4M, K100M	172–175N	N-60K, 303	98N	No	Maggi et al. (2000)
2	HPMC > PEO	Texture analysis	6.8 pH phosphate	9.5 mm/6.5 mm <sup>b</sup>	K15M, K100LV	78N	301	137N	Glipizide	Jamzad and Fasshi (2006)
3	PEO > HPMC	Texture analysis	DI water	3.2 mm/2.5 mm <sup>c</sup>	K100LV, K4M, K15M	N/A	205, N012K, N60K, COAG	N/A	No	Yang et al. (1998)
4	HPMC > PEO	Micro-indentation	1.2 pH HCl/KCl	5 mm/3 mm <sup>d</sup>	K100M	259N	301	329N	No	

<sup>a</sup> Tablet volume.

<sup>b</sup> Tablet thickness.

<sup>c</sup> Gel layer thickness at 4 h.

<sup>d</sup> Tablet thickness at 7 h.

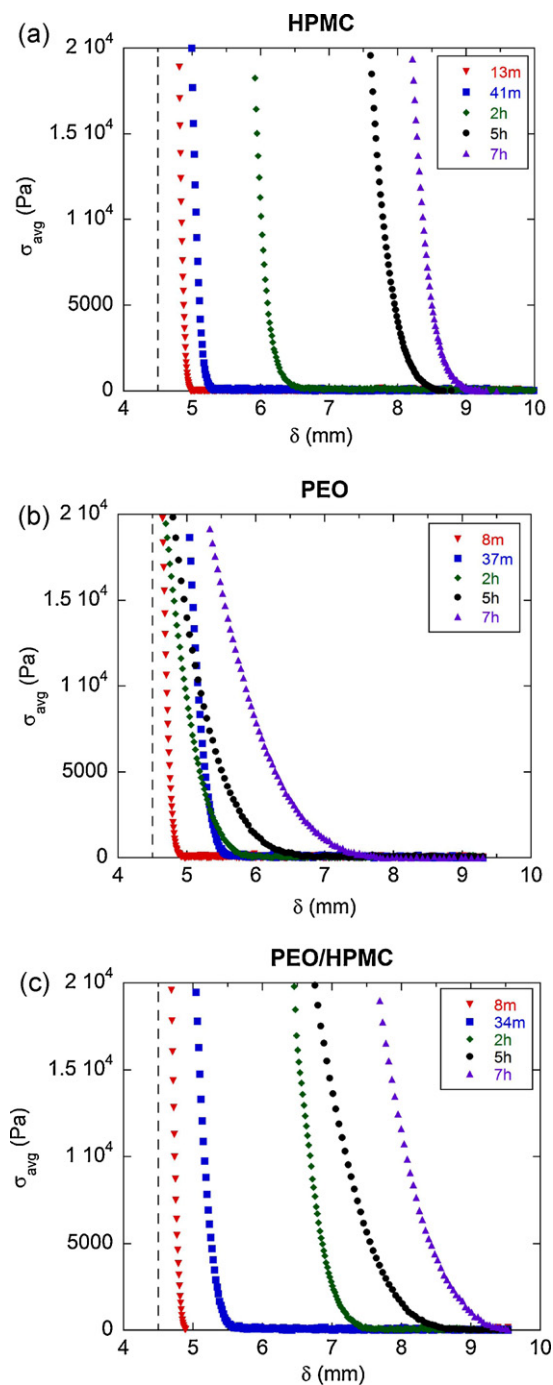


**Fig. 8.** Select curves showing stress as a function of indenter displacement for (a) HPMC, (b) PEO, and (c) PEO/HPMC. The dashed line represents the surface of the dry compact.

In other studies, gravimetric measurements provide swelling in terms of weight only and do not account for differences in axial or radial expansion of a compact or matrix. The indentation experiments, by contrast, are only sensitive to swelling in the axial direction. Visual observation of the PEO compact during hydration exhibited both radial and axial swelling, while the HPMC swelled primarily in the axial direction. The blended compact exhibited axial swelling comparable to the pure HPMC compact. Its radial swelling was observed to be less than the PEO compact, but greater than HPMC. These differences in swelling behavior warrant future investigation and may be affected by particle morphology and degrees of freedom after compaction.

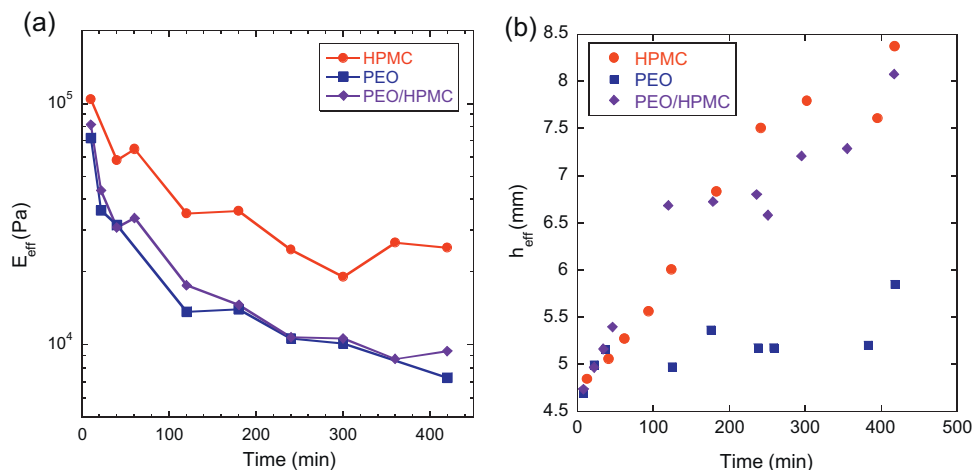


Fig. 9. Effective modulus (a) and thickness (b) data for all three samples as a function of swelling time.

### 3.2. Elastic modulus

The HPMC compact has a fairly consistent stress response during 7 h of swelling. This consistency implies that the gel structure is not changing drastically with an increased degree of swelling. This is likely due to the hydrophobic regions of the chains that collapse during hydration. These collapsed regions reduce chain motility and help maintain the structure and mechanical integrity of the gel over time. The PEO compact, by contrast, shows a distinct softening after approximately 2 h. After this point, the indenter must travel a greater distance to reach the same stress level. This softening corresponds to hydration of the inner core of the compact. As expected, the gel stiffness decreases as the chains become more hydrated. Because these matrices are not cross-linked, the stiffness of the gel layer is dependent upon the number of entanglements between chains, which decreases as the gel swells. As the increasingly mobile chains disentangle they are then free to migrate into solution. The reduction in swelling as compared to the HPMC compact may also be reflective of this gel dissolution. Yang et al. observed a similar decrease in slope during texture analysis measurements of PEO compacts (Yang et al., 1998). Efentakis et al. reported a swelling plateau for PEO compacts around 1–3 h, followed by a rapid decrease of the glassy core (Efentakis et al., 2007). The time scale observed in their experiment corresponds to the time during which we begin to see pronounced softening in our samples. The HPMC/PEO blend compact also shows some softening after 2 h. In this case we see behavior from both of the component materials. The presence of HPMC reduces the degree of softening that occurs relative to the pure PEO compact. The HPMC seems to dominate the behavior at short times in addition to the degree of

overall swelling, while the PEO promotes the ingress of solution and hydration of the inner core of the compact.

Fig. 9 shows the effective moduli of the three types of compacts as a function of hydration time. The data were taken from the experiments depicted in Fig. 8; each line represents swelling data from a single compact. The effective modulus of the HPMC gradually decreases to 25–40 kPa. This plateau region is likely due to the physical cross-links formed by hydrophobic regions of the chains. The initial decrease in modulus is attributed to swelling of the chains from the glassy core. At longer times the outer layers of chains have reached a limit of swelling and the physical cross-links control the response. The PEO modulus decreased from 36 to 7 kPa as the outer layer of chains became less dense. Unlike the HPMC compact, this sample did not reach a plateau in the modulus during the time frame of the experiments. The effective modulus decreases as the PEO chains continually disentangle and migrate into solution. The presence of PEO appears to dominate the hybrid compact response at all times. The blend compact modulus remains slightly higher than that of the PEO sample, but the longer-term stability of the HPMC chains is overwhelmed by the dissolution of the gel layer due to the PEO chain migration.

### 3.3. Oscillatory indentation

Oscillatory indentation experiments were conducted on compacts that were immersed in room-temperature deionized water for 6 h. Results showed that the HPMC compact's complex modulus,  $E^*$ , decreased from approximately 2 MPa to 0.18 MPa after 6 h of immersion (Fig. 10a). The PEO and PEO/HPMC blend compacts' moduli decreased from 1.3 MPa to 0.17 MPa and 1.6 MPa to 0.3 MPa,

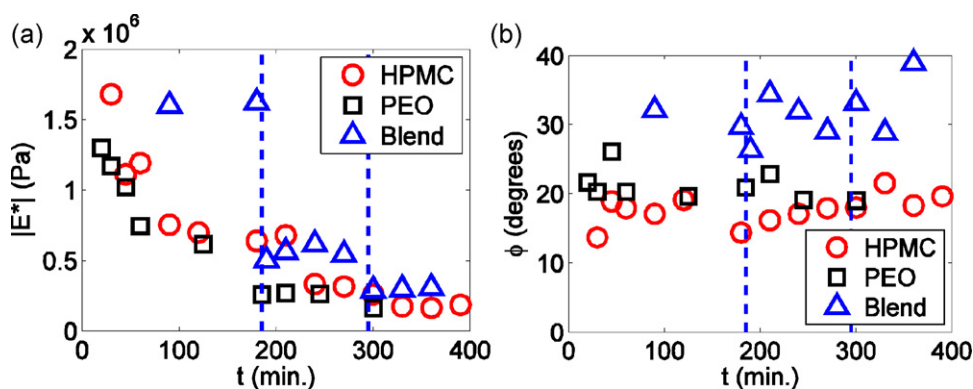


Fig. 10. Complex modulus (a) and phase angle (b) data for the three compacts as a function of hydration time. Data were obtained at an oscillation frequency of 1 Hz.

respectively, over the same time frame. These results are two orders of magnitude larger than the calculated effective modulus values. The difference between the results can be attributed to the stress levels at which the moduli were calculated. The effective modulus was defined at a stress of 10 kPa while the oscillatory indentation modulus is being calculated over a higher range of stresses, from 30 to 225 kPa. The dashed lines in Fig. 10 represent regions in which all samples were tested at the same initial stress. In the first region the samples were tested at 50 mN (113 kPa), in the second region at 25 mN (57 kPa), and the third at 15 mN (34 kPa). Because the properties of the gel layer vary with thickness, the calculated modulus values are dependent upon the stress, and thus the depth at which the measurements are taken. At shorter times the complex modulus of the HPMC and PEO compacts gradually decrease while the blend compact remains constant. At longer times the complex moduli of all three compacts remain fairly constant. In this last regime the inner region of the gel has reached its equilibrium swollen state but has not yet begun to dissolve. Additionally, during the indentation portion of the experiment prior to oscillation, the indenter may be compacting the region of gel directly beneath it. This compression may also give rise to a larger modulus value since the chains beneath the punch are more dense than in their equilibrium state.

While the detailed results obtained from the indentation measurements clearly depend on the detailed loading history, some important distinctions between the different formulations is immediately evident from the data in Fig. 10. For example, the viscoelastic phase angle at 1 Hz is consistently largest for the blend formulation, indicating that this sample exhibits the most significant stress relaxation over a 1-s time scale. Overall, these experiments demonstrate the potential for using these tests to provide information about the evolution of the viscoelastic behavior of the gel layer during the swelling process.

#### 4. Conclusions

Traditional texture analysis measures both the axial swelling and gel strength of a compact or matrix, but it is a destructive test that results in fracture of the sample. The indentation technique described here measures both axial swelling and gel mechanical properties using a non-destructive method that allows for continuous measurement of the same compact. Measurements of HPMC, PEO, and HPMC/PEO compacts showed that the technique is sensitive to changes in compact thickness and mechanical response and can be used to characterize changes in the mechanical properties of the gel during the swelling process. Defining an effective elastic modulus provides a general way to compare sample behavior, while oscillatory indentation experiments have provided a technique for conducting small-scale rheological experiments to measure the evolution of viscoelastic behavior of the gel layer as it swells. The technique can easily be extended to more complex systems of directly clinical relevance, aiding in the development of more effective drug delivery vehicles by increasing our understanding of matrix behavior in multi-layer or drug-containing systems.

#### Acknowledgment

This work was supported through the National Science Foundation through Grant CMMI-0900586.

#### References

Abrahmsen-Alami, S., Korner, A., Nilsson, I., Larsson, A., 2007. New release cell for NMR microimaging of tablets. Swelling and erosion of poly(ethylene oxide). *Int. J. Pharm.* 342, 105–114.

- Adler, J., Jayan, A., Melia, C.D., 1999. A method for quantifying differential expansion within hydrating hydrophilic matrixes by tracking embedded fluorescent microspheres. *J. Pharm. Sci.* 88, 371–377.
- Chen, Y.Y., Hughes, L.P., Gladden, L.F., Mantle, M.D., 2010. Quantitative ultra-fast MRI of HPMC swelling and dissolution. *J. Pharm. Sci.* 99, 3462–3472.
- Colombo, P., Bettini, R., Peppas, N.A., 1999. Observation of swelling process and diffusion front position during swelling in hydroxypropyl methyl cellulose (HPMC) matrices containing a soluble drug. *J. Control. Release* 61, 83–91.
- Conti, S., Maggi, L., Segale, L., Machiste, E.O., Conte, U., Grenier, P., Vergnault, G., 2007a. Matrices containing NaCMC and HPMC. 1. Dissolution performance characterization. *Int. J. Pharm.* 333, 136–142.
- Conti, S., Maggi, L., Segale, L., Machiste, E.O., Conte, U., Grenier, P., Vergnault, G., 2007b. Matrices containing NaCMC and HPMC. 2. Swelling and release mechanism study. *Int. J. Pharm.* 333, 143–151.
- Crosby, A.J., Shull, K.R., Lin, Y.Y., Hui, C.Y., 2002. Rheological properties and adhesive failure of thin viscoelastic layers. *J. Rheol.* 46, 273–294.
- Durig, T., Fassihi, R., 2002. Guar-based monolithic matrix systems: effect of ionizable and non-ionizable substances and excipients on gel dynamics and release kinetics. *J. Control. Release* 80, 45–56.
- Efentakis, M., Pagoni, I., Vlachou, M., Avgoustakis, K., 2007. Dimensional changes, gel layer evolution and drug release studies in hydrophilic matrices loaded with drugs of different solubility. *Int. J. Pharm.* 339, 66–75.
- Formulary, U.S.P.a.N., 2009. United States Pharmacopeia Convention, Rockville, MD.
- Gall, T.P., Lasky, R.C., Kramer, E.J., 1990. Case II diffusion. Effect of solvent molecule size. *Polymer* 31, 1491–1499.
- Harland, R.S., Gazzaniga, A., Sangalli, M.E., Colombo, P., Peppas, N.A., 1988. Drug/polymer matrix swelling and dissolution. *Pharm. Res.* 5, 488–494.
- Jamzad, S., Tutunji, L., Fassihi, R., 2005. Analysis of macromolecular changes and drug release from hydrophilic matrix systems. *Int. J. Pharm.* 292, 75–85.
- Jamzad, S., Fassihi, R., 2006. Development of a controlled release low dose class II drug-Glipizide. *Int. J. Pharm.* 312, 24–32.
- Ju, R.T.C., Nixon, P.R., Patel, M.V., 1995. Drug-release from hydrophilic matrices. 1. New scaling laws for predicting polymer and drug-release based on the polymer disentanglement concentration and the diffusion layer. *J. Pharm. Sci.* 84, 1455–1463.
- Kavanagh, N., Corrigan, O.I., 2004. Swelling and erosion properties of hydroxypropylmethylcellulose (Hypromellose) matrices – influence of agitation rate and dissolution medium composition. *Int. J. Pharm.* 279, 141–152.
- Laity, P.R., Cameron, R.E., 2010. Synchrotron X-ray microtomographic study of tablet swelling. *Eur. J. Pharm. Biopharm.* 75, 263–276.
- Laity, P.R., Mantle, M.D., Gladden, L.F., Cameron, R.E., 2010. Magnetic resonance imaging and X-ray microtomography studies of a gel-forming tablet formulation. *Eur. J. Pharm. Biopharm.* 74, 109–119.
- Li, H.T., Gu, X.C., 2007. Correlation between drug dissolution and polymer hydration: a study using texture analysis. *Int. J. Pharm.* 342, 18–25.
- Lin, W.-C., Otim, K.J., Lenhart, J.L., Cole, P.J., Shull, K.R., 2009. Indentation fracture of silicone gels. *J. Mater. Res.* 24, 957–965.
- Maggi, L., Bruni, R., Conte, U., 2000. High molecular weight polyethylene oxides (PEOs) as an alternative to HPMC in controlled release dosage forms. *Int. J. Pharm.* 195, 229–238.
- Maggi, L., Segale, L., Torre, M.L., Machiste, E.O., Conte, U., 2002. Dissolution behaviour of hydrophilic matrix tablets containing two different polyethylene oxides (PEOs) for the controlled release of a water-soluble drug. Dimensionality study. *Biomaterials* 23, 1113–1119.
- Mikac, U., Sepe, A., Kristl, J., Baumgartner, S., 2010. A new approach combining different MRI methods to provide detailed view on swelling dynamics of xanthan tablets influencing drug release at different pH and ionic strength. *J. Control. Release* 145, 247–256.
- Reynolds, T.D., Gehrke, S.H., Hussain, A.S., Shenouda, L.S., 1998. Polymer erosion and drug release characterization of hydroxypropyl methylcellulose matrices. *J. Pharm. Sci.* 87, 1115–1123.
- Ridgway, K., 1970. Aspects of pharmaceutical engineering. *Pharm. J.*, 709–712.
- Ritscher, T.A., Elias, H.G., 1959. The problem of the membrane during osmotic measurements on high polymers III. *Makromol. Chem.* 30, 38–80.
- Shull, K.R., 2002. Contact mechanics and the adhesion of soft solids. *Mater. Sci. Eng. R: Rep.* 36, 1–45.
- Shull, K.R., Ahn, D., Chen, W.-L., Flanigan, C.M., Crosby, A.J., 1998. Axisymmetric adhesion tests of soft materials. *Macromol. Chem. Phys.* 199, 489–511.
- Sneddon, I.N., 1965. The relation between load and penetration in the axisymmetric Boussinesq problem for a punch of arbitrary profile. *Int. J. Eng. Sci.* 3, 47–57.
- Sung, K.C., Nixon, P.R., Skoug, J.W., Ju, T.R., Gao, P., Topp, E.M., Patel, M.V., 1996. Effect of formulation variables on drug and polymer release from HPMC-based matrix tablets. *Int. J. Pharm.* 142, 53–60.
- Thomas, N., Windle, A.H., 1978. Transport of methanol in poly(methyl methacrylate). *Polymer* 19, 255–265.
- Wan, L.S.C., Heng, P.W.S., Wong, L.F., 1995. Matrix swelling – a simple model describing extent of swelling of HPMC matrices. *Int. J. Pharm.* 116, 159–168.
- Wu, N., Wang, L.S., Tan, D.C.W., Mochhala, S.M., Yang, Y.Y., 2005. Mathematical modeling and in vitro study of controlled drug release via a highly swellable and dissoluble polymer matrix: polyethylene oxide with high molecular weights. *J. Control. Release* 102, 569–581.
- Yang, L.B., Johnson, B., Fassihi, R., 1998. Determination of continuous changes in the gel layer thickness of poly(ethylene oxide) and HPMC tablets undergoing hydration: a texture analysis study. *Pharm. Res.* 15, 1902–1906.